Nanoscale

ELECTRONIC SUPPLEMENTARY MATERIAL

Thin Film Synthesis of SbSI Micro-Crystals for Self-Powered Photodetectors with Rapid Time Response

Karl C. Gödel,[a] and Ullrich Steiner*[b]

[a] *Cavendish Laboratory, Department of Physics, University of Cambridge, J J Thomson Avenue, Cambridge CB3 0HE, United Kingdom.*
[b] *Adolphe Merkle Institute, Rue des Verdiers, CH-1700 Fribourg, Switzerland. E-mail: ullrich.steiner@unifr.ch*

Fig. 1 Photograph of an amorphous Sb_2S_3 sample and a SbSI sample after conversion with SbI_3 and rinsing in ethanol.

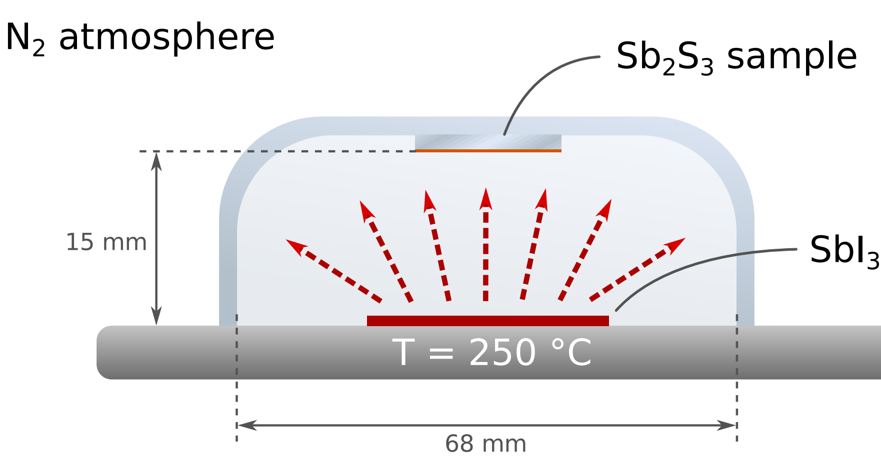

Fig. 2 Schematic of the evaporation procedure to convert amorphous Sb_2S_3 to crystalline SbSI. The conversion process is complete after only 15 min.

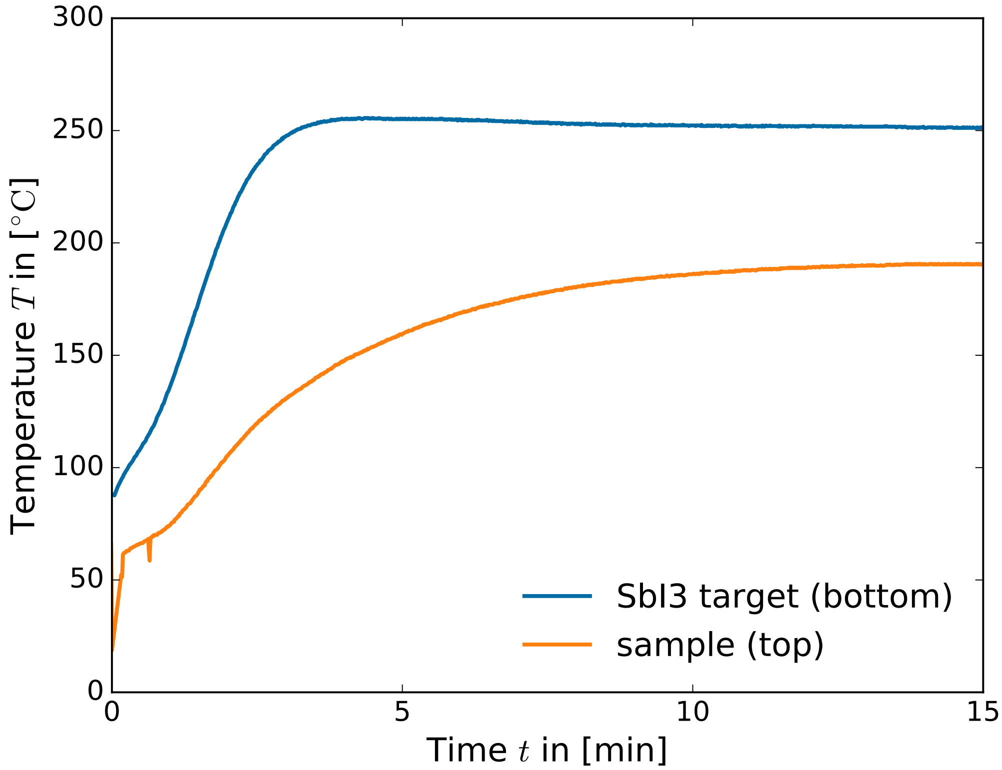

Fig. 3 Temperature curve of the SbI_3 target on the hot plate (blue), and the sample at the top of the reaction chamber (yellow). The temperatures were measured using a Pt100 temperature sensor.

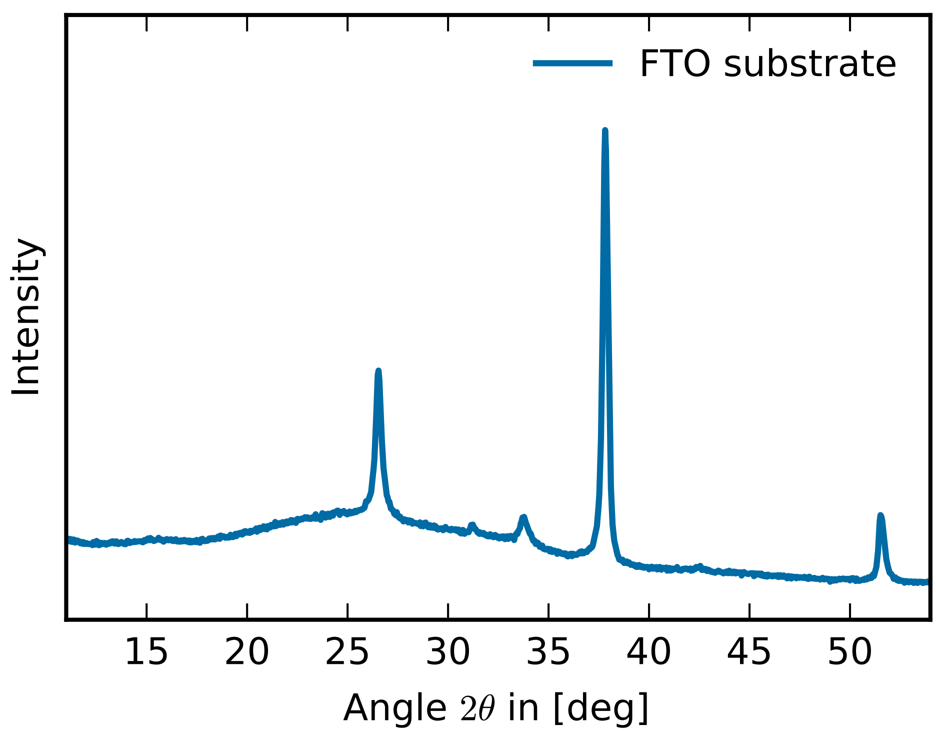

Fig. 4 XRD reference of a FTO-glass substrate.

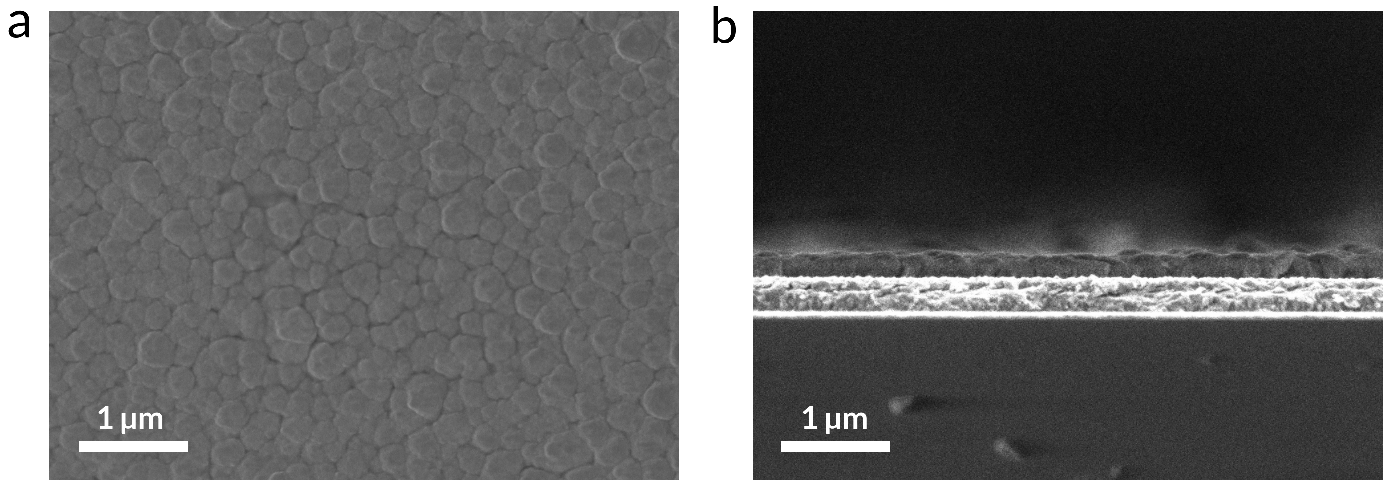

Fig. 5 (a) Top and (b) cross-sectional SEM images of an initial amorphous Sb_2S_3 layer on a FTO substrate.

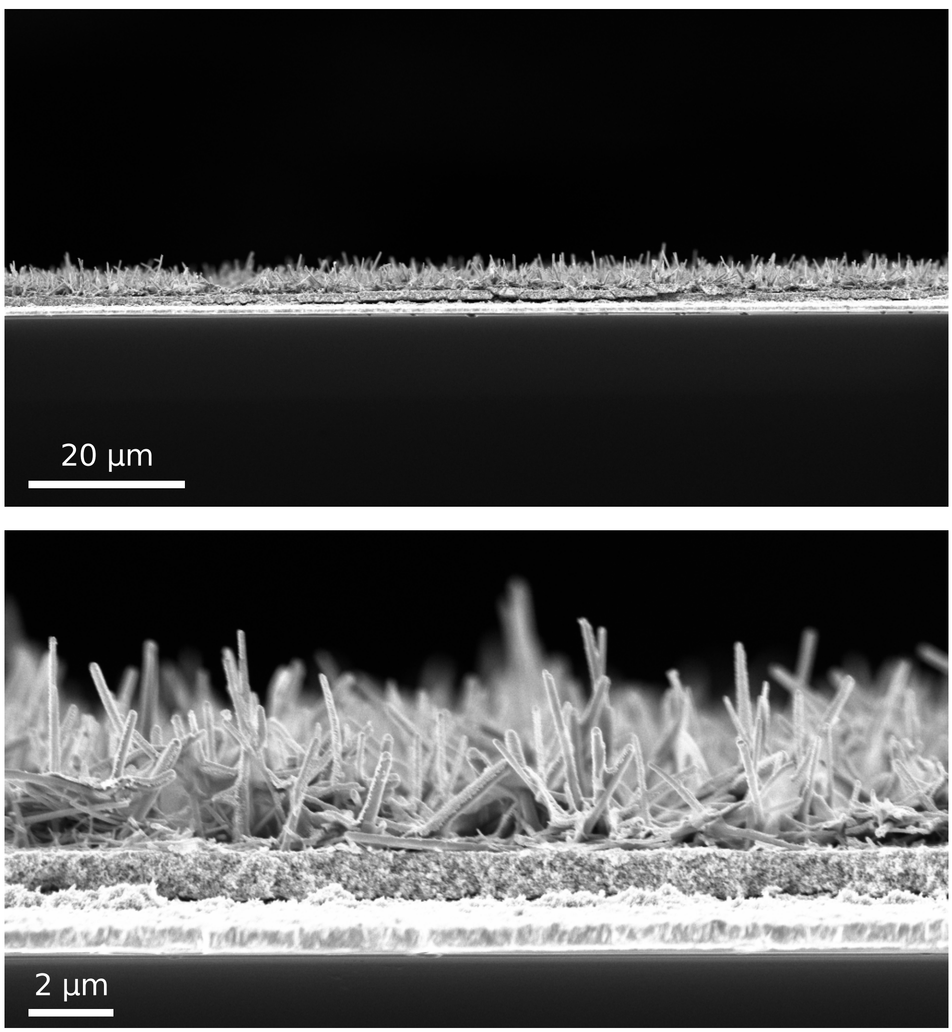

Fig. 6 Cross-sectional SEM micrographs showing the preferential orientation of SbSI crystal needles perpendicular to the substrate surface. Note that these samples had an additional mesoporous ITO layer that was deposited onto the FTO substrate prior to the formation of SbSI. This additional layer is however not necessary and was omitted in the characterised photodetectors.

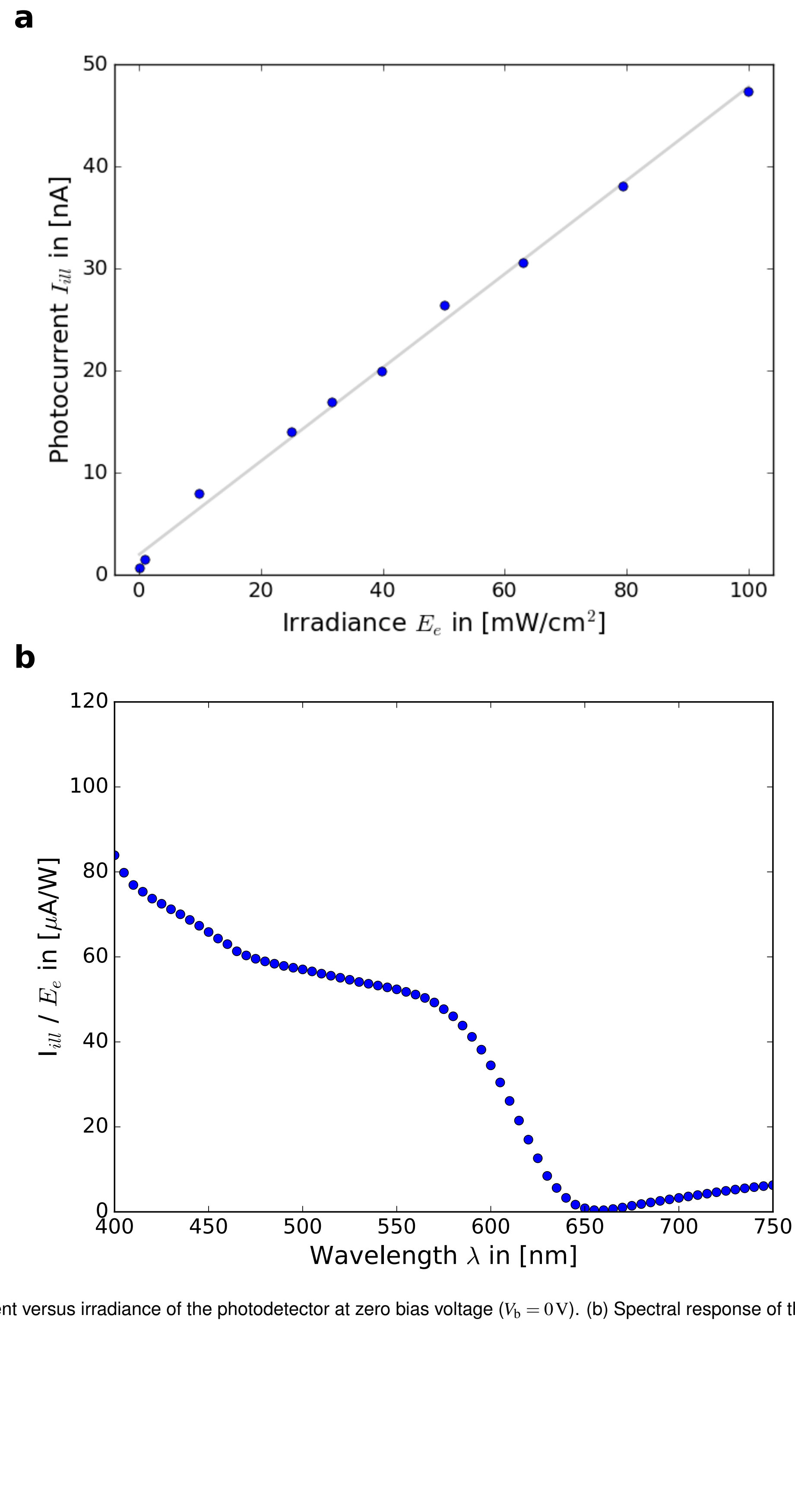

Fig. 7 (a) Photocurrent versus irradiance of the photodetector at zero bias voltage ($V_b = 0\,V$). (b) Spectral response of the photodetector at $V_b = 0\,V$.

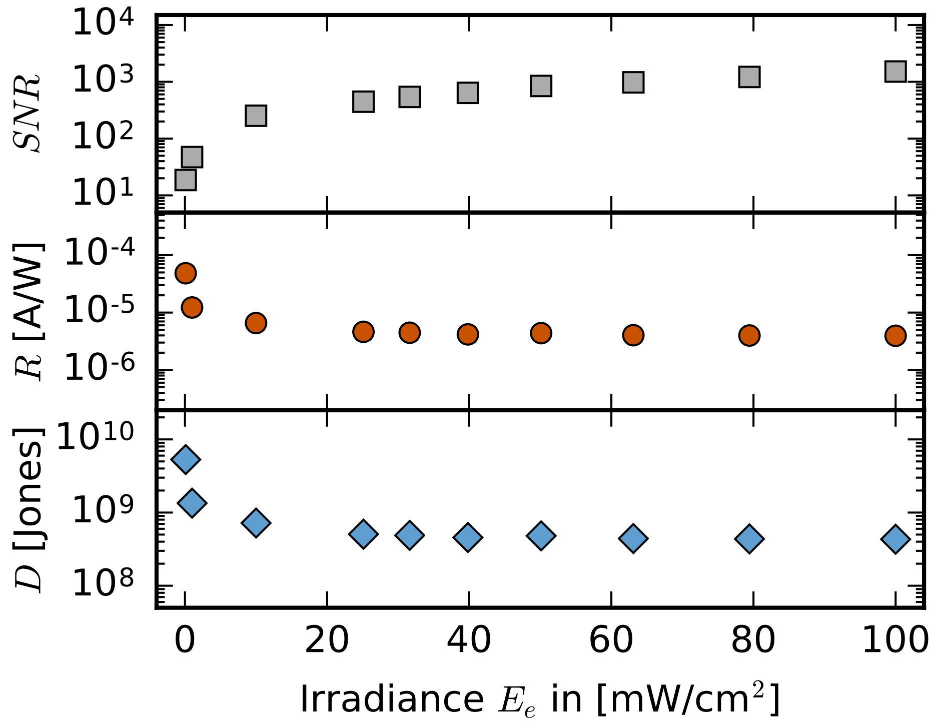

Fig. 8 Signal-to-noise ratio SNR, responsivity R and specific detectivity D^* as a function of the illumination irradiance E_e at zero bias $V_b = 0\,V$.

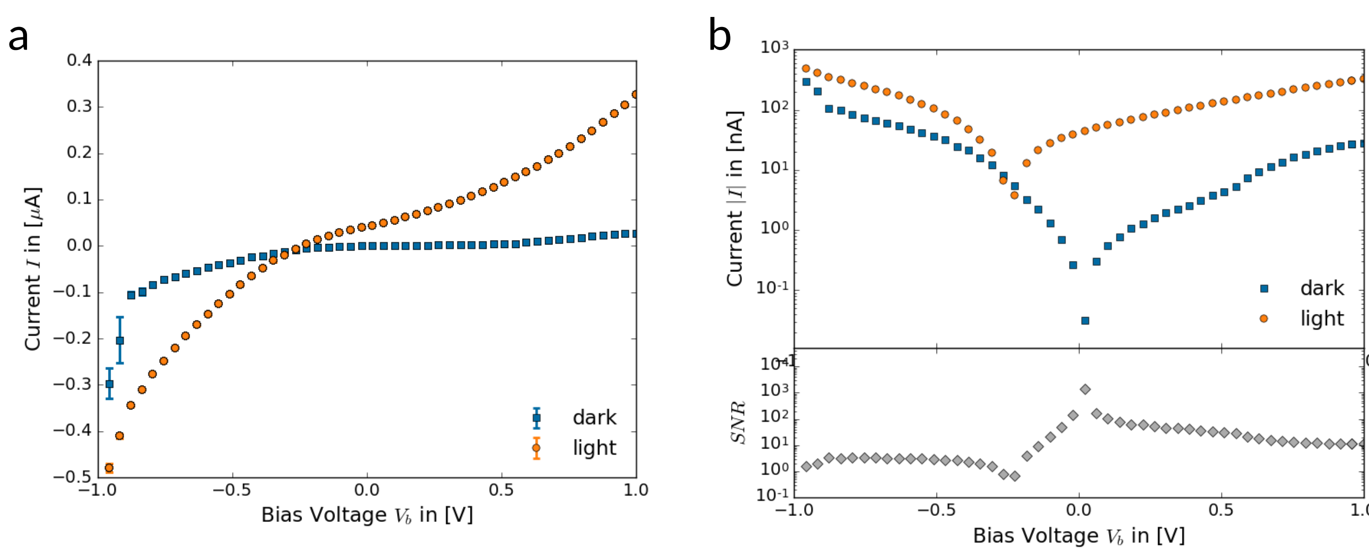

Fig. 9 (a) Linear and (b) logarithmic plot of the dark- and photocurrent of the photodetector for different bias voltages V_b. The lower frame shows corresponding signal-to-noise ratios SNR. The SNR is highest for low bias voltages, due to the low dark currents.

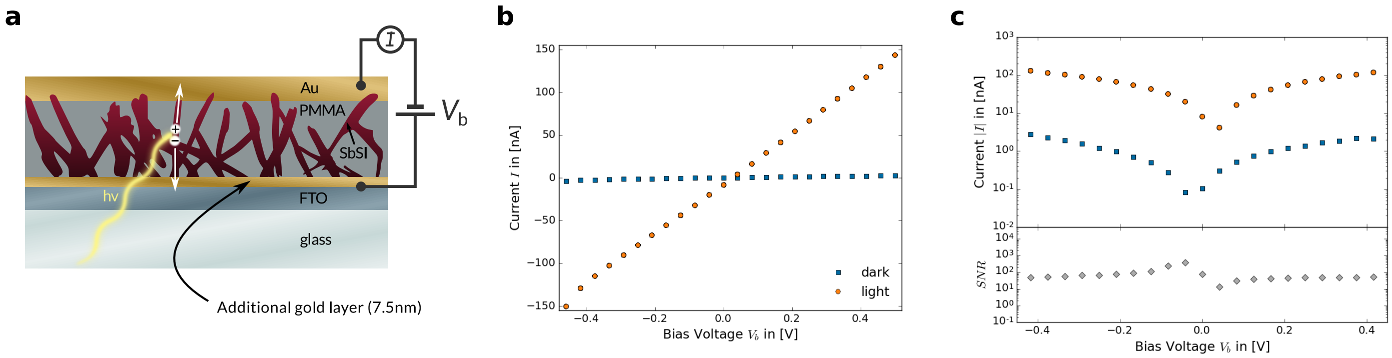

Fig. 10 (a) Schematic drawing of a photodetector incorporating an additional layer of gold (thickness 7.5 nm) on top of the FTO electrode, demonstrating the effect of symmetrical electrode work functions, compared to asymmetric work functions in Figures **??** and 9. (b) Dark- and photocurrent of the photodetector with the additional gold layer as a function of bias voltages V_b. (c) Logarithmic plot of the same measurement. The lower frame shows the corresponding signal-to-noise ratios *SNR*.

Table 1 Comparison of the figures of merit of SbSI, perovskite-based and a high performance CdSe-nanowire photodetector

Photodetector	I_{light} [a]	*SNR*	Detectivity D^*	Rise time τ_r	Fall time τ_f	Reference
"sandwich" SbSI	54 nA	1373	$6.8 \cdot 10^9$	8 ms	34 ms	This work
single-crystal SbSI	$\approx$ 1.8 nA	700	$\approx 2.3 \cdot 10^9$	300 ms	300 ms	[1]
Perovskite ($CH_3NH_3PbI_3$)	$\approx$ 10 nA	92	—	1200 ms	200 ms	[2]
CdSe-nanowire [b]	—	10^7	$4 \cdot 10^{13}$	350 ns	350 ns	[3]

[a] $V_b = 0.1\,V, E_e = 100\,\frac{mW}{cm^2}$, [b] No self-powered mode possible.

References

1 G. Chen, W. Li, Y. Yu and Q. Yang, *RSC Advances*, 2015, **5**, 21859–21864.

2 H. Lu, W. Tian, F. Cao, Y. Ma, B. Gu and L. Li, *Advanced Functional Materials*, 2016, **26**, 1296–1302.

3 A. Littig, H. Lehmann, C. Klinke, T. Kipp and A. Mews, *ACS Applied Materials & Interfaces*, 2015, **7**, 12184–12192.